

MS.4.P106

Electron microscopy study of Yttrium-doped $\text{Ba}_{0.5}\text{Sr}_{0.5}\text{Co}_{0.8}\text{Fe}_{0.2}\text{O}_{3-\delta}$

M. Meffert^{1,2}, P. Müller^{1,2}, H. Störmer¹, C. Niedrig³, S.F. Wagner³, E. Ivers-Tiffée^{3,2}, D. Gerthsen^{1,2}

¹Karlsruher Institut für Technologie, Laboratorium für Elektronenmikroskopie, Karlsruhe, Germany

²Karlsruher Institut für Technologie, DFG Center for Functional Nanostructures, Karlsruhe, Germany

³Karlsruher Institut für Technologie, Institut für Werkstoffe der Elektrotechnik, Karlsruhe, Germany

matthias.meffert@kit.edu

Keywords: BSCF, Yttrium-doping, perovskite

ABO₃-type perovskite oxides have been identified as promising materials for application in oxygen separation membranes. Among these perovskites $\text{Ba}_{0.5}\text{Sr}_{0.5}\text{Co}_{0.8}\text{Fe}_{0.2}\text{O}_{3-\delta}$ (BSCF) has received particular attention due to its exceptional high oxygen permeation properties. However, a major obstacle for the application is the thermodynamic instability of the cubic BSCF phase at application-relevant temperatures. The desired cubic phase decomposes at temperatures below 900 °C, resulting in a slow decrease of oxygen flux making it unsuitable for long-term operation. It is assumed that the decomposition is initiated by the decreasing concentration of oxygen vacancies with decreasing temperature which requires an increase of the valence of the B-site cations to preserve overall charge neutrality. This leads to a change of the ionic radius of the B-site cations and a corresponding destabilization of the cubic BSCF phase. Therefore, the cubic phase decomposes into various secondary phases, like the hexagonal BSCF phase, Co-oxide, precipitates with plate-like morphology, which are composed of thin lamellae of the cubic and hexagonal phases, and barium cobaltites $\text{Ba}_{n+1}\text{Co}_n\text{O}_{3n+3}(\text{Co}_8\text{O}_8)$ with $n \geq 2$ (denoted BCO) [1-4].

To improve the long-term stability of the cubic BSCF phase B-site doping with monovalent transition metals was investigated. Recent studies show improved phase stability for Zr-doped BSCF with a dopant concentration as low as 3 at% [5]. Furthermore, Y-doped BSCF has been reported to even improve considerably the oxygen conductivity [6]. However, a detailed phase investigation with high spatial resolution is still missing. Therefore, undoped and Y-doped BSCF was investigated by transmission electron microscopy and scanning electron microscopy (SEM). Electron energy loss spectroscopy (EELS) was applied to study the valence of the Co-cations. Energy dispersive X-ray spectroscopy (EDXS) was used for composition analysis.

Y-doped BSCF powder was prepared using the mixed-oxide route. Mixed raw powders were calcined and isostatically pressed into compacts. After sintering and homogenization, the bulk samples were annealed at temperatures from 700 °C to 900 °C for 100 h in ambient air. Prior to the SEM investigation the bulk samples were polished up to a surface roughness of about 0.1 µm, followed by an etching process using a colloidal silicon dioxide suspension. Due to the different etching rates of the different BSCF phases, a surface topography develops resulting in secondary electron contrast. This contrast can be directly related to the different BSCF phases [3], which allows a quick large-scale characterization of the phase composition of numerous samples.

Figure 1 shows SEM images of etched (a) undoped and (b) 3 at% Y-doped BSCF bulk samples after annealing at 700 °C. Undoped BSCF contains a large volume fraction of secondary phases, mainly precipitates with plate-like morphology surrounded by the hexagonal phase with dark contrast as shown in Fig. 1(a). Furthermore, CoO precipitates could be observed. In contrast, Y-doped BSCF only shows the hexagonal phase which can be found exclusively at grain boundary regions (dark contrast in Fig. 1(b)). After 800 °C annealing, the hexagonal phase is only formed at triple points of grain boundaries in Y-doped BSCF. At 900 °C, secondary phases were not detected in Y-doped BSCF whereas undoped BSCF contains BCO-type lamellae and CoO grains. Therefore, Y strongly reduces the concentration of nucleation centers for the hexagonal phase compared to undoped BSCF. However, Y does not fully suppress the formation of the hexagonal phase. Therefore, chemical analyses were performed to gain further insights into the decomposition process. EDXS mappings of a region containing the cubic BSCF phase and the hexagonal phase at a grain boundary (Figure 2) show a strong increase of Co and a depletion of Fe and Y whereas the Ba- and Sr-concentrations (mappings not shown here) only change marginally. The lack of Y in the hexagonal phase might be one reason for the improved phase stability because the formation of secondary phases requires a strong diffusion of B-site cations which might be suppressed by the large ionic radius of Y³⁺.

Since the change of the Co-valence plays a major role in the decomposition process, the Co-valence state was investigated by EELS. Since the Ba-M_{4,5} white-lines are superimposed on the Co-

L_{2,3} white-lines, Co-valence determination cannot be performed by the measurement of the Co-L_{2,3} white-line intensity ratio. Therefore, a new method was developed to characterize the Co-valence state in BSCF by determining the change in Co-L_{2,3} white-line distance. This technique was elaborated on the basis of Co-L_{2,3} white-line distance measurements of reference materials with known Co-valence state. This method allows to easily map the Co-valence over a comparably large region as shown in Figure 3(a). The corresponding sample area of the mapping is marked with a white frame in the HAADF-STEM image Figure 3(b). Figure 3(a) confirms the supposed different Co-valence states in the hexagonal and cubic phase. In the cubic phase of Y-doped BSCF the valence of cobalt is about 2+, whereas in the hexagonal phase the valence state of cobalt is elevated ($\geq 2.6+$).

1. S. Švarcová et al, SSI 178 (2008) p. 1787.
2. C. Niedrig et al, SSI 197 (2011) p. 25.
3. P. Müller et al, SSI 206 (2012) p. 57.
4. P. Müller et al, Chem. Mater. 25 (2013) p. 564.
5. S. Yakovlev et al, Appl. Phys. Lett. 96 (2010) p. 254 101.
6. P. Haworth et al, Sep. Purif. Technol. 81 (2011) p. 88.
7. This work has been performed within the project F.2 of the DFG Research Center for Functional Nanostructures (CFN). It has been further supported by a grant from the Ministry of Science, Research and the Arts of Baden-Württemberg (Az: 7713.14-300) and by the Helmholtz Association of German Research Centres through the portfolio topic MEM-BRAIN.

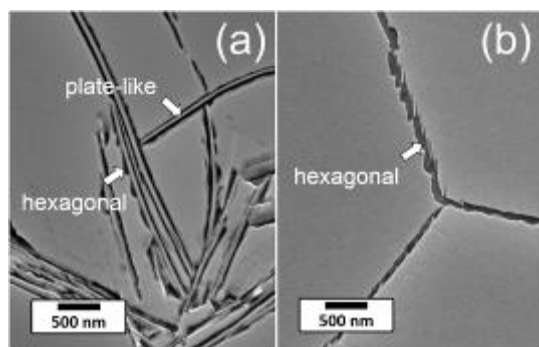


Figure 1. SEM micrographs of etched (a) undoped and (b) 3 at% Y-doped BSCF annealed at 700 °C for 100 h. The dark contrast corresponds to the hexagonal phase.

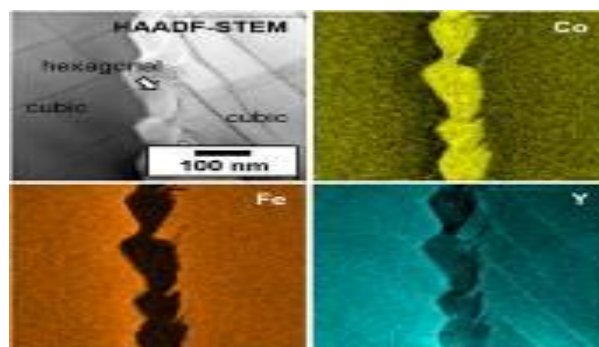


Figure 2. EDXS mappings of the Co-, Y- and Fe-distribution in cubic BSCF and hexagonal BSCF at a grain boundary in 3 at% Y-doped BSCF annealed at 700 °C for 100 h.

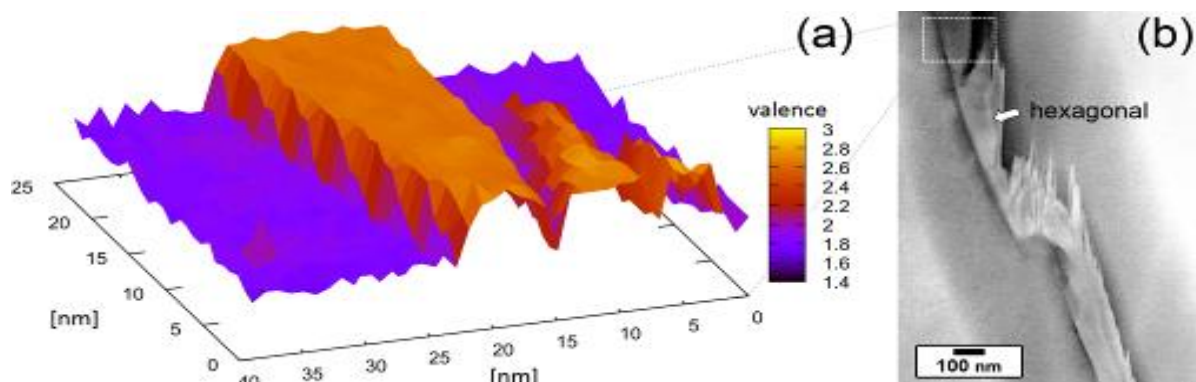


Figure 3. (a) EELS Co-valence mapping of a grain boundary region containing the hexagonal phase in 3 at% Y-doped BSCF annealed at 730 °C for 100 h. (b) Overview HAADF-STEM image. The white frame corresponds to the sample area where the Co-valence mapping was performed.